Optimal PWM Based on Real-Time Solution of Harmonic Elimination Equations

Jian Sun, *Member, IEEE,* Stephan Beineke, and Horst Grotstollen

Abstract—**Pulse-width modulation (PWM) based on the elimination of low-order harmonics necessitates solving systems of nonlinear equations. Conventional implementations of this technique based on storing off-line calculated solutions have the common problem that the system flexibility is very limited, especially for applications that require both amplitude and frequency control. A new implementation scheme based on real-time solution of nonlinear harmonic elimination equations using a digital signal processor DSP56001 is reported in this paper. With this digital signal processor (DSP), optimal pulse patterns having 15 switching angles in each quarter fundamental period can be determined within 2.15 ms. Details of the system hardware and software are described. New theoretical results concerning the solvability of harmonic elimination equations are also presented.**

I. Introduction

PULSE-WIDTH modulation (PWM) of dc/ac power inverters has been the subject of intensive investigations in the past two decades [1]. At low to medium power levels, simple modulation methods are desirable for limiting system complexity and cost. Transient response at these power levels is usually also of great concern. In addition, the relatively low power rating permits the use of power switches that can be operated at high switching frequency such that satisfactory waveforms can be generated without having to optimize each individual switching instant. In this context, various carrier-based PWM methods are well suited for low- and medium-power applications due to their moderate requirements on the hardware for implementation, good transient response, and well-defined waveform spectrums when the ratio of switching frequency to the fundamental frequency is large [2].

A. Optimal Pulse-Width Modulation

At a high power level, to limit switching losses power switches (e.g., GTO's) can only be switched at low frequencies (typically several hundred hertz). This implies that only a few switching actions may take place within each fundamental period, as far as the fundamental frequency is not very low. In this case, optimizing the waveform based on specifying an optimal value for each switching instant is necessary for achieving the best modulation result. The high power and cost of the whole system also justify the use of such optimized modulation methods that, in principle, require more advanced (thus more expensive) implementation hardware and software than that of simple carrier-based PWM. The benefits of optimization are also more remarkable, considering the total power of the system.

As the total energy of harmonics contained in a PWM waveform is constant that depends only on the fundamental amplitude, regardless of the actual waveform structure, optimizing the waveform implies not eliminating or reducing the total harmonic energy, but altering its distribution among different frequency components. Considering that most electrical as well as mechanical systems feature some kind of low-pass characteristics, low-order harmonics are usually considered to be more harmful than high-order ones, thus they need to be controlled at smaller magnitudes. Hence, roughly speaking, the objective of optimal PWM is to push most harmonic energy into high-frequency regions such that low-frequency harmonics are well attenuated.

B. Harmonic Elimination

One frequently studied optimal PWM method is the harmonic elimination technique, which aims at the complete elimination of some low-order harmonics [3]–[7]. The underlying principle of harmonic elimination is that the fundamental and harmonic amplitudes of a symmetrical PWM waveform are nonlinear functions of the N switching angles in the first quarter fundamental period. Setting the fundamental amplitude to a pre-specified value and other $N-1$ low-order harmonics to zero results in a system of N nonlinear equations. The desired optimal pulse patterns can thus be determined by solving these equations. Two major advantages of applying this technique are:

1) If the inverter is used to supply ac power of constant frequency to general ac loads, a filter is usually installed at its output. In this case, when low-order harmonics are eliminated through the modulation of the inverter, only high-order harmonics will appear at the output and need to be attenuated by the filter. The cut-off frequency of the filter can thus be increased, leading to a significant reduction of the filter size. System efficiency also tends to increase.
2) When used in an ac drive system, eliminating the low-order harmonic voltages leads to great reduction of low-order harmonic torques generated by the motor. Although harmonic torque is the results of interacting between stator and rotor harmonic currents of different orders, higher-order harmonic currents have smaller magnitudes due to the larger impedance that the motor

Manuscript received November 11, 1994; revised January 8, 1996.

The authors are with the Institute for Power Electronics and Electrical Drives, Electrical Engineering Department, University of Paderborn, 33098 Paderborn, Germany.

Publisher Item Identifier S 0885-8993(96)05158-7.

presents to higher-order harmonic voltages. Their contributions to lower-order harmonic torques are thus less significant. Lower-order harmonic torques generated by the motor are thus greatly reduced.

C. Conventional Implementation Schemes

Due to the high complexity, solving harmonic elimination equations on-line during real-time operation has been considered impractical, and all implementation schemes reported so far are based on solving first the equations off-line [6], [7]. The results are then either directly stored in look-up tables or interpolated by simple functions for real-time operation.

For high-power applications, in order to maintain a constant switching frequency such as to limit switching losses, the ratio of the switching frequency f_s to the fundamental frequency f_1 has to be reduced when the fundamental frequency increases. This implies that it is necessary to solve harmonic elimination equations both for variable fundamental amplitude, which is necessary for regulating output voltage, and for different numbers of switching angles to control the output frequency while keeping the switching frequency constant. The look-up table for storing off-line calculated solutions will occupy much memory space, hence making the system inflexible and difficult to maintain. This is especially the case for applications such as ac motor drives, which require both magnitude and frequency control.

Real-time generation of switching angles from simple functions that approximate off-line calculated solution trajectories would avoid the use of large memory, thus improving the flexibility and maintenance of the system. The accuracy of the on-line-generated switching angles depends on the proximity of functions and could be increased, at least theoretically, to any extent by using, say, high-order polynomials. However, this is true only when frequency control is not required. For variable frequency operations, considering the fact that the number of switching angles in each fundamental period has to be adjusted during real-time operation to maintain a constant switching frequency, many approximate functions have to be stored. This leads to the same problem as when the off-line-calculated solutions are directly stored in look-up tables.

Therefore, conventional implementation schemes for the harmonic elimination technique based on off-line-calculated solutions and using either look-up tables or approximate functions method are not effective for practical applications that require both voltage and frequency control, such as for ac drives. The problem could be tackled by solving harmonic elimination equations directly on-line in real-time. However, although digital technology has undergone very rapid advances in recent years and many sophisticated digital devices are available today, solving harmonic elimination equations in real time has still been considered impractical.

A new implementation scheme based on real-time solution of nonlinear harmonic elimination equations using a digital signal processor DSP56001 is reported in this paper. The paper is organized as follows. Different waveform structures and the corresponding harmonic elimination equations are introduced in Section II. Algorithms for effectively solving these equations and the question of whether their Jacobian matrix is singular are then discussed in Section III. An overview of the hardware system for the proposed new implementation scheme is provided in Section IV. Details of assembly programs implemented in the DSP56001 for accomplishing the on-line solution are described in Section V. Section VI illustrates then various experimental results. Finally, Section VII concludes the paper and points out some directions for future studies.

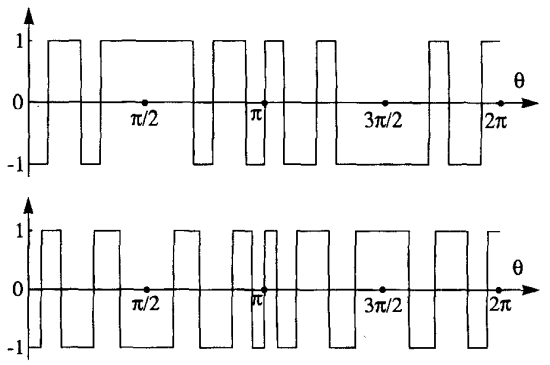

Fig. 1. Structural alternatives of two-level PWM waveforms.

II. Waveforms and Equations

Only two-level line-to-neutral (LN) voltage waveforms are considered in this paper. To ensure the absence of even-order harmonics, each waveform is assumed to be quarter-period symmetrical and half-period inversely symmetrical. The waveform is normalized by half of the dc-link voltage such that it has two discrete levels: $+1$ and -1. The maximal fundamental amplitude of such a waveform thus is $4\pi^{-1}$, which is achieved when no modulation takes place in each half-wave period.

Two basic structural alternatives of two-level PWM waveforms to be studied in this paper are shown in Fig. 1. They will be referred to as LN1 and LN2 waveforms. For single- and three-phase applications, they are denoted further as SLN1, SLN2, TLN1, and TLN2, respectively.

A. Waveform Representation

A symmetrical PWM waveform with a given structure will be uniquely determined if the N switching angles in the first quarter period are specified. Evidently, these angles must satisfy the basic constraint

$$0 \le \alpha_1 \le \alpha_2 \le \cdots \le \alpha_{N-1} \le \alpha_N \le \frac{\pi}{2}. \tag{1}$$

For each waveform, we use a $(N+1)$-dimensional vector $\boldsymbol{h} = [h_0, h_1, h_2, \cdots, h_N]^T$ to represent its initial level at $\theta = 0$ and the variation of levels at all N switching instants. That is

$$\boldsymbol{h} = [-1, 2, -2, \cdots, 2]^T \text{ for LN1 waveforms}$$
$$\boldsymbol{h} = [1, -2, 2, \cdots, 2]^T \text{ for LN2 waveforms.}$$

Based on these notations, Fourier representation of a PWM waveform introduced above can be easily determined to be

$$f(\theta) = \sum_{k=0}^{\infty} V_{2k+1} \sin\left[(2k+1)\theta\right] \tag{2}$$

where V_{2k+1} is the amplitude of the $(2k+1)$th harmonic voltage $(k = 0, 1, 2, \cdots)$

$$V_{2k+1} = \frac{4}{(2k+1)\pi}\left[h_0 + \sum_{i=1}^{N} h_i \cos\left[(2k+1)\alpha_i\right]\right]. \tag{3}$$

B. Harmonic Elimination Equations

Harmonic elimination aims at the elimination of $N-1$ low-order harmonics from the output of an inverter while regulating its fundamental amplitude at a pre-specified value M. Considering the absence of even-order harmonics, the harmonics to be eliminated are normally the $N-1$ lowest odd-order ones for single-phase inverters. For three-phase inverters, since triple-order harmonics do not have any effect on the load, only the $N-1$ lowest odd-order nontriple harmonics need to be eliminated. Thus, in a general form, harmonic elimination equations may be written as

$$V_1 = M: \quad h_0 + \sum_{i=1}^{N} h_i \cos\alpha_i - \frac{\pi M}{4} = 0$$

$$V_k = 0: \quad h_0 + \sum_{i=1}^{N} h_i \cos\left(k\alpha_i\right) = 0$$

where $k = \{3, 5, \cdots, 2N-1\}$ for SLN1 and SLN2 waveforms, $\{5, 7, \cdots, 3N-2\}$ for TLN1 waveforms, and $\{5, 7, \cdots, 3N-1\}$ for TLN2 waveforms. These equations may be formally denoted as

$$\boldsymbol{g}(\boldsymbol{a}) = \boldsymbol{0}, \quad \boldsymbol{a} = [\alpha_1, \alpha_2, \cdots, \alpha_N]^T. \tag{4}$$

For example, for the LN1 waveform shown in Fig. 2, the system of harmonic elimination equations (for single-phase inverters) are

$$\begin{aligned} -1 + 2\cos\alpha_1 - 2\cos\alpha_2 + 2\cos\alpha_3 - \frac{\pi M}{4} &= 0 \\ -1 + 2\cos 3\alpha_1 - 2\cos 3\alpha_2 + 2\cos 3\alpha_3 &= 0 \\ -1 + 2\cos 5\alpha_1 - 2\cos 5\alpha_2 + 2\cos 5\alpha_3 &= 0. \end{aligned} \tag{5}$$

III. Off-Line Solution

A. Algorithms for Off-Line Solution

Newton's method may be applied to solve harmonic elimination equations (4). For a given value of M, this method solves the equations iteratively in the following sequence:

1) generating an initial guess of solution as the starting point: $\boldsymbol{a}^{(k)}, k = 0$;
2) formulating a local linear model

$$\boldsymbol{J}(\boldsymbol{a}^{(k)})\Delta\boldsymbol{a}^{(k)} + \boldsymbol{g}(\boldsymbol{a}^{(k)}) = \boldsymbol{0}; \tag{6}$$

3) solving the local linear model (6) for $\Delta\boldsymbol{a}^{(k)}$;
4) updating: $\boldsymbol{a}^{(k+1)} = \boldsymbol{a}^{(k)} + \Delta\boldsymbol{a}^{(k)}$; $k = k+1$, return to 2).

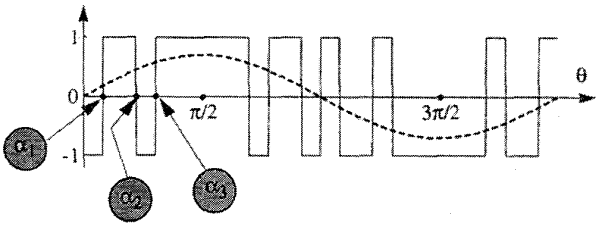

Fig. 2. A symmetrical PWM waveform.

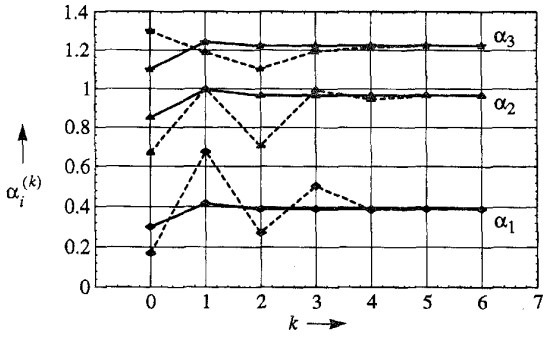

Fig. 3. The convergence of Newton's method starting from $\boldsymbol{a}^{(0)} = [0.3, 0.85, 1.1]^T$ (solid lines) and $\boldsymbol{a}^{(0)} = [0.17, 0.67, 1.3]^T$ (dashed lines).

In (6), $\boldsymbol{J}(\boldsymbol{a})$ is the Jacobian matrix of $\boldsymbol{g}(\boldsymbol{a})$, which, for the example equations system (5), is

$$\boldsymbol{J}(\boldsymbol{a}) = \begin{bmatrix} -2\sin\alpha_1 & -2\sin\alpha_2 & -2\sin\alpha_3 \\ -6\sin 3\alpha_1 & -6\sin 3\alpha_2 & -6\sin 3\alpha_3 \\ -10\sin 5\alpha_1 & -10\sin 5\alpha_2 & -10\sin 5\alpha_3 \end{bmatrix}.$$

The convergence of Newton's method when applied to solve (5) with $M = 0.5$ is illustrated in Fig. 3 for two starting points: $\boldsymbol{a}^{(0)} = [0.3, 0.85, 1.1]^T$ and $\boldsymbol{a}^{(0)} = [0.17, 0.67, 1.3]^T$. The corresponding exact solution is $\boldsymbol{a} = [0.3895, 0.9664, 1.2243]^T$. As can be seen, this solution is obtained after only a few iterations.

B. The Starting Points

Apparently, the successful application of Newton's method to harmonic elimination equations depends on whether

1) a good starting point $\boldsymbol{a}^{(0)}$ can be provided for each required fundamental amplitude, and
2) the Jacobian matrix $\boldsymbol{J}(\boldsymbol{a})$ is nonsingular with $\boldsymbol{a} = \boldsymbol{a}^{(k)}$ at each iteration k.

Novel algorithms for the generation of starting points have been proposed in [8] and [10]. They are based on solving the equations first for zero output voltage ($M = 0$, is called the "null solution") and then using various continuation methods to extend the solution to nonzero output. The proposed continuation methods include zero-order prediction, linear extrapolation (Euler prediction), and the continuous differential equations approach. Using these methods, starting points that are close enough to the exact solution to ensure the convergence of Newton's method can be generated for different output voltages.

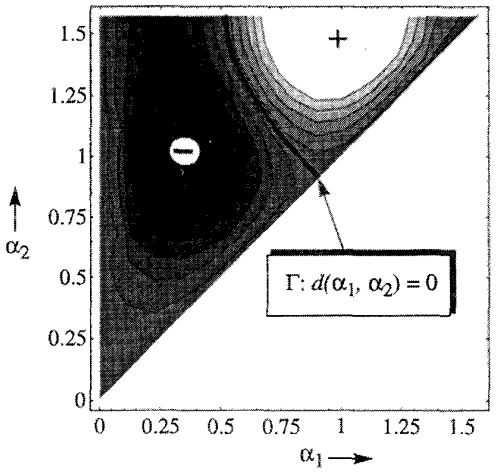

Fig. 4. Contour plot of function $d(\alpha_1, \alpha_2)$ for $0 < \alpha_1 < \alpha_2 \leq \pi/2$.

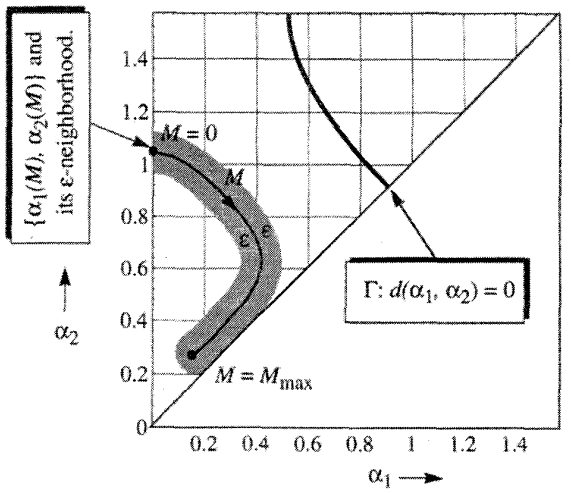

Fig. 5. The trajectory of solutions to (8) and its ε-neighborhood for variable M.

C. The Jacobian Matrix

The second question raised above is answered by the following theorem for single-phase inverters:

Theorem: For single-phase inverters, as far as LN1 and LN2 waveforms are considered, the Jacobian matrix $\boldsymbol{J}(\boldsymbol{a})$ of harmonic elimination equations $\boldsymbol{g}(\boldsymbol{a}) = 0$ is nonsingular if and only if the N switching angles $\alpha_1, \alpha_2, \cdots, \alpha_{N-1}$ and α_N are positive and distinct from each other, that is

$$0 < \alpha_1 < \alpha_2 < \cdots < \alpha_{N-1} < \alpha_n \leq \frac{\pi}{2}. \tag{7}$$

Proof of this theorem is given in the Appendix. For three-phase inverters, however, a similar result can not be justified: the Jacobian matrix $\boldsymbol{J}(\boldsymbol{a})$ may become singular even if the condition (7) is satisfied by N switching angles. To demonstrate this, a TLN2 waveform with $N = 2$ is considered. Harmonic elimination equations for this waveform are

$$\begin{aligned} 1 - 2\cos\alpha_1 + 2\cos\alpha_2 - \frac{\pi M}{4} &= 0 \\ 1 - 2\cos 5\alpha_1 + 2\cos 5\alpha_2 &= 0 \end{aligned} \tag{8}$$

and their Jacobian matrix is

$$\boldsymbol{J}(\alpha_1, \alpha_2) = \begin{bmatrix} 2\sin\alpha_1 & -2\sin\alpha_2 \\ 10\sin 5\alpha_1 & -10\sin 5\alpha_2 \end{bmatrix}.$$

To show that this matrix may become singular for $0 < \alpha_1 < \alpha_2 \leq \pi/2$, its determinant $d(\alpha_1, \alpha_2) = \det \boldsymbol{J}(\alpha_1, \alpha_2)$ is calculated to be

$$d(\alpha_1, \alpha_2) = 20(\sin\alpha_2 \sin 5\alpha_1 - \sin\alpha_1 \sin 5\alpha_2).$$

It is easy to check that the function $d(\alpha_1, \alpha_2)$ vanishes for $\alpha_1 = 0.6$ and $\alpha_2 = 1.305\,35$; that is, $d(0.6, 1.305\,35) = 0$. The matrix $\boldsymbol{J}(\alpha_1, \alpha_2)$ is thus singular at this point. To see if $\boldsymbol{J}(\alpha_1, \alpha_2)$ becomes singular also at other points, a contour plot of $d(\alpha_1, \alpha_2)$ is provided in Fig. 4. As can be seen, $d(\alpha_1, \alpha_2)$ vanishes not at some discrete points, but in a continuous curve denoted by Γ.

However, the fact that $\boldsymbol{J}(\alpha_1, \alpha_2)$ is singular along the curve Γ does not necessarily imply that harmonic elimination equations (8) can not be solved in this case. In fact, the solution to (8) has been calculated for M varying from 0 to $M_{\max}$ and its trajectory has been plotted in Fig. 5. This is explained below.

The convergence of Newton's method guarantees that for any M, if the starting point $\boldsymbol{a}^{(0)}$ belongs to an ε-neighborhood ($\varepsilon \ll 1$) of the exact solution $\boldsymbol{a}^*$, then each iterative solution $\boldsymbol{a}^{(k)}$ lies also inside this neighborhood and will converge to $\boldsymbol{a}^*$. On the other hand, using a proper off-line solution algorithm as developed in [8] and mentioned in the last subsection, a starting point can be provided for each M using either a zero-order or an Euler predictor. Thus, by increasing M each time by a small amount ΔM, it is possible to generate a starting point that lies inside the ε-neighborhood of the exact solution $\boldsymbol{a}^*$. Since the solution trajectory is well separated from the curve Γ, its ε-neighborhood does not intersect with Γ even when e is as large as 0.6, as can be seen from Fig. 5. The occurrence of a singular Jacobian matrix $\boldsymbol{J}$ during the off-line calculation of solution trajectories can thus be avoided.

For the case that there are more variables ($N > 2$), it can be inferred that the points at which the Jacobian matrix $\boldsymbol{J}$ becomes singular constitute a $(N-1)$-dimensional subset Γ of the solution space $D \subset R^N$. The solvability of harmonic elimination equations depends thus on whether there exists an $\varepsilon > 0$ such that the ε-neighborhood of the solution trajectory does not intersect with Γ. As has been confirmed by our experience, this is indeed the case for at least all TLN1 and TLN2 waveforms.

D. Solution Trajectories

Using the solution algorithms discussed so far, harmonic elimination equations with different unknown variables and for variable M can be solved. As an illustration, Fig. 6 shows the variation of solutions with M for a TLN1 waveform with $N = 5$. The maximum modulation index $M_{\max}$ in this case is 1.17, above which no harmonic elimination solution exists. It is to be observed from this and the previous results that

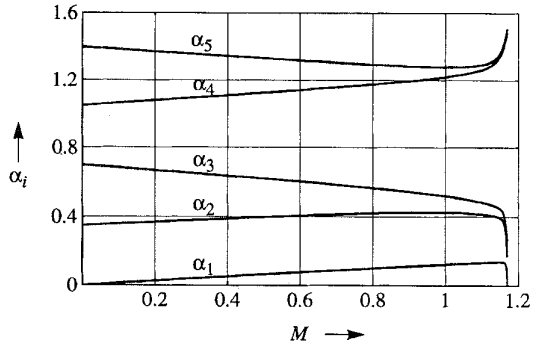

Fig. 6. Trajectories of harmonic elimination solutions for variable output voltage.

1) the switching angles vary fairly linearly with M over a large portion of the inverter operating range, and
2) Newton's algorithm converges at the exact solution after a few $(2 \sim 3)$ iterations, even when an very inaccurate starting point is used.

The first observation indicates that solution trajectories for variable M can be well approximated by simple (even linear) functions. The second one implies that if such approximate functions are evaluated for a given M to generate a starting point, exact solutions could be obtained after very few iterations using Newton's method. This suggests that the following harmonic elimination technique could be implemented in real-time.

1) Off-line calculated solutions are first approximated by simple functions of the fundamental output voltage.
2) These functions, together with harmonic elimination equations and Newton's method for solving the equations, are implemented on a DSP.
3) During real-time operation, the DSP generates first an approximate solution in accordance with the required output M through the evaluation of the stored functions, uses it as the starting point, and runs the Newton's algorithm to find the exact solution.

A DSP-based real-time harmonic elimination system following this scheme will be presented in the next sections.

IV. Overview of the Hardware System

Referring to Fig. 7, the operating principle of the implemented experimental system is as follows: The host computer in a workstation (NeXT) simulates a voltage controller and generates a voltage reference M. The DSP56001 reads once in each sampling period the reference voltage, solves the system of harmonic elimination equations, and then outputs the resulting switching angles to the interface box. The switching angles are then converted into a sequence of switching pulses in the interface box and are sent to the drive circuit of the inverter through optical fibers.

A. The DSP56001

The Motorola DSP56001 [9] is a 24-bit general purpose digital signal processor that features 512 words of full-speed on-chip program RAM, two independent 256×24-bit data

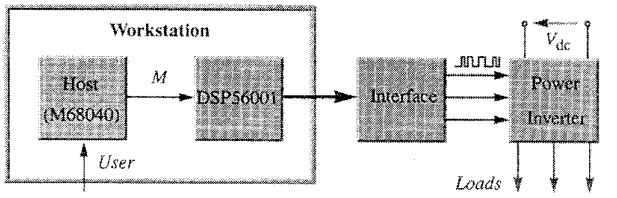

Fig. 7. Hardware system for on-line solution of harmonic elimination equations.

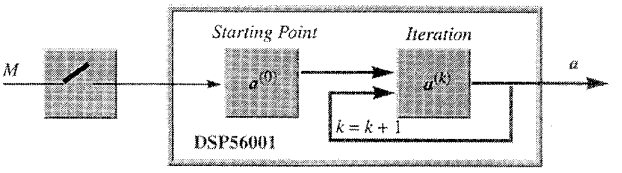

Fig. 8. Principle flow chart of assembly programs in the DSP.

RAM's, and two preprogrammed data ROM's (one of which is factory programmed with a full sine wave table). In our experimental system this DSP is clocked at 25 MHz, at which each instruction cycle takes 80 ns. It is connected to the host through its general purpose I/O Port B. Outside the workstation, the DSP can be accessed through its synchronous serial interface (SSI) and serial communication interface (SCI) pins that are combined in a D-15 connector.

The major function of the DSP is to solve harmonic elimination equations on-line during real-time operation. Similar to off-line calculations, the equations are solved by using Newton's method and this is accomplished in several steps (see Fig. 8).

1) The reference voltage M provided by the host computer is sampled at the beginning of each half fundamental period of the inverter output.
2) Approximate switching angles are generated from a set of simple linear functions in accordance with the sampled reference voltage M. The coefficients of the linear functions have been determined in advance from off-line calculation results and are stored in the DSP at the initialization stage of the system.
3) Using the approximate switching angles as the starting point, an iterative solution algorithm is started to calculate the exact solution iteratively.
4) The calculated angles are fed to the hardware interface. The DSP waits then for the next sampling period.

Details of algorithms implemented in the DSP are described in the next section.

B. The Generation of Pulse Sequence Using a XC4005

The hardware peripheries in the interface box are built around the XC4005 (XILINK™), a field programmable logic cell array with 196 configurable logic blocks, 616 flip-flops, and 112 input/output blocks. It is configured to create from the optimal switching angles received from the DSP a corresponding sequence of switching pulses. Outside the XC4005, an auxiliary circuitry is designed to convert the electrical pulse

signals into optical ones and to feed them through optical fibers to the drive circuits of inverter power switches.

The configuration program for the XC4005 is first prepared using its specific development tools. Configuration is then accomplished at the initialization stage of the system by writing the configuration data file from NeXT workstation through DSP56001 to XC4005.

C. The Host Computer

The host computer (M68040 CPU) serves multiple functions: At the development stage of the system, it provides an environment for the preparation of assembly programs of the DSP. An object-oriented simulation program is also developed for verifying the function of the assembly programs before using them to control a real power inverter. The simulation is carried out in such a way that after having solved the system of nonlinear harmonic elimination equations, the DSP56001 sends back the calculated switching angles to the host computer where they can be analyzed and compared with previously calculated exact solutions.

An initialization process is invoked whenever the hardware system is to be started. At this stage, the host computer defines first the function of XC4005 by sending it a configuration program. Afterwards, main assembly programs of the DSP, coefficients of linear functions from which the DSP generates the starting point for its iterative solution program, and other necessary initial data are sent to the DSP56001 where they are stored in the internal program and data RAM's, respectively. The system is then ready for operation.

During real-time operation, the host computer simulates a voltage controller and provides a reference voltage for the DSP. Dynamic response of the whole modulation system may thus be investigated through the generation of various reference signals (step-wise, sinusoidal, or random sequences) in the host computer.

V. DSP Assembly Programs

Compact and efficient assembly programs of the DSP are essential to the success of the new on-line solution scheme and are at the center of the work. This is a very challenging task if one considers, on the one hand, the high complexity of harmonic elimination equations that are to be solved by the DSP and, on the other hand, the very critical time requirement for achieving real-time operation of the modulation system. The key features of the assembly programs that we have developed are described below.

A. The Generation of Starting Points

As mentioned before, for a sampled value of M the DSP first generates a set of approximate solution angles through the evaluation of some simple linear functions and then applies Newton's method to find the exact solution iteratively. These linear functions have been determined in advance based on the least-square approximation of off-line calculated solution trajectories. Their coefficients are then stored in the data RAM of the DSP during the initialization stage.

It must be pointed out that approximating each individual solution trajectory by one linear function has the disadvantage that many linear functions will have to be stored for realizing variable frequency control. For instance, if N varies from 2 to 16, one needs to store $2+3+\cdots+16=135$ linear functions; that is, 270 constant coefficients. To avoid this, the method proposed in [5] has been applied to establish some uniform approximate functions that are valid for variable number of switching angles.

The approximation method is based on the observation that, at $M=0$, the solution trajectories start from regularly distributed points (the null solution). If the approximate functions are imposed to pass these points, then only their slopes need yet to be determined. This can be done in three steps, as proposed in [5].

1) A slope m_i is determined for each angle α_i individually.
2) The slopes of angles that decrease with M are averaged to give an average positive slope m_p. An average negative slope m_n is determined likewise.
3) For variable N, the average positive and negative slopes are interpolated, respectively, using the least-square method. This gives two functions $m_p(N)$ and $m_n(N)$.

Then, for a certain N, with functions $m_p(N)$ and $m_n(N)$, the approximate function for α_i is $\alpha_i(M)\approx\alpha_i^{(0)}+m_p(N)M$ if α_i increases with M, and $\alpha_i(M)\approx\alpha_i^{(0)}+m_n(N)M$ if α_i decreases with M, $\alpha_i^{(0)}$ being the null solution of α_i at $M=0, i=1,2,\cdots,N$.

For example, functions $m_p(N)$ and $m_n(N)$ for TLN1 waveforms are determined in [5] as

$$m_p(N)=5.0391e^{-0.071\,25N}$$
$$m_n(N)=-6.4384e^{-0.056\,72N}.$$

As given in [10], for $N=5$, the null solution for this type of waveforms is

$$\alpha_1=0,\quad \alpha_2=\frac{\pi}{9},\quad \alpha_3=\frac{2\pi}{9},\quad \alpha_4=\frac{\pi}{3},\quad \alpha_5=\frac{4\pi}{9}.$$

In addition, it is also known that α_1 and α_2 increase with M, while α_{2i+1} decreases, $i=1,2,\cdots,(N-1)/2$. This information can be easily programmed in the DSP, with which starting points can be generated for any given N and M. For comparison, both the exact solution trajectories and such determined linear approximate functions for the considered TLN1 waveform are illustrated in Fig. 9 by the solid and dashed lines, respectively. To see how Newton's method will converge from a starting point determined using such approximate functions, the number of iterations necessary to achieve the required accuracy of 0.1° for each solution angle is illustrated in Fig. 10. As can be seen, for most $M\in[0,M_{\max}]$, one or two iterations are sufficient.

Considering that the reference M does not change very often during normal operation, the following procedures are used in the DSP for the determination of a starting point.

1) If the sampled value of M in the current sampling period is very close to that of the last period, i.e., $|M_{k+1}-M_k|\le\delta$, δ being a small positive real number,

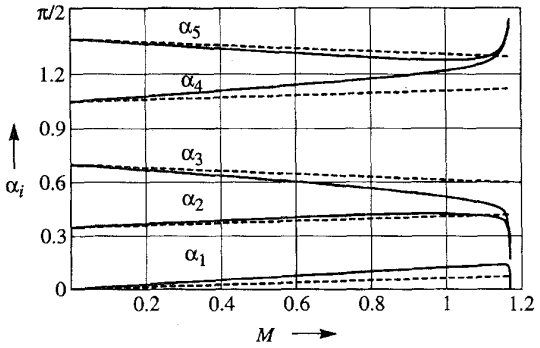

Fig. 9. Comparison between the exact solution trajectories (solid lines) and their approximation by linear functions (dashed lines).

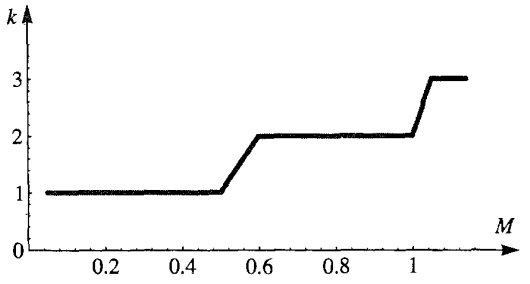

Fig. 10. Number of Newton's iterations for achieving the required accuracy of 0.1°.

then the solution calculated for the last M is taken directly as the new starting point.

2) Otherwise, the stored linear functions are evaluated to generate a new starting point.

This will remove the steady-state error from the solution and is analogous to having an integrator in the control loop of the modulation system. It also improves the convergence of the solution algorithm when M varies slowly.

B. Formulation of the Local Linear Model

Whenever a starting point has been determined, an iterative program based on Newton's method is executed in the DSP to find the exact solution. Similar to off-line solution procedures outlined in Section II, each iteration in the DSP comprises two major steps:

1) formulating a local linear model: $\boldsymbol{J}(\boldsymbol{a})\Delta\boldsymbol{a} + \boldsymbol{g}(\boldsymbol{a}) = 0$;
2) solving the local linear model and updating the iterative solution.

The algorithm used to solve the local linear model in the DSP is a direct implementation of the Gauss elimination method. Details of this part are thus omitted.

The formulation of the local linear model is one of the most time-consuming tasks that the DSP has to perform. This is due to the presence of $2N^2$ trigonometric functions in the model.[1] To reduce the total computation time, algorithms used to evaluate these trigonometric functions must be very efficient. This has been achieved based on using the preprogrammed 256-word sine wave table, which is located at the Y data memory of the DSP, occupying locations 256 through 511. That is, the value of $\sin(m360°/256)$ can be found from the $256 + m$ location of Y data memory. An angle $\alpha \in [0, 360°)$ may thus be decomposed into the addition of two parts as

$$\alpha = m(360°/256) + \Delta\alpha = \alpha_{(m)} + \Delta\alpha.$$

Using Taylor expansions, $sin\ \alpha$ and $cos\ \alpha$ can be approximately calculated from

$$\sin(\alpha) \approx [1 - 0.5(\Delta\alpha)^2]\sin\alpha_{(m)} + \Delta\alpha\cos\alpha_{(m)} \quad (9)$$

$$\cos(\alpha) \approx [1 - 0.5(\Delta\alpha)^2]\cos\alpha_{(m)} - \Delta\alpha\sin\alpha_{(m)}. \quad (10)$$

Because $\cos\alpha_{(m)} = \sin(90° + \alpha_{(m)}) = \sin\alpha_{(m+64)}$, values of both $\sin\alpha_{(m)}$ and $\cos\alpha_{(m)}$ are directly available form the sine wave table when m is known.

To effectively generate the corresponding integer m and fraction $\Delta\alpha$ for an angle α, the data format has been designed in such a way that, when α is stored in a 24-bits data memory, the first eight most significant bits (MSB) as an integer is equal to m, and the fraction amount represented by the remaining bits corresponding to $\Delta\alpha$. Therefore, both m and $\Delta\alpha$ are obtained once by shifting the binary representation of α by 8 bits to the left.

C. Gauss Elimination and Dynamical Scaling

As the DSP56001 supports only fixed-point arithmetic instructions, the local linear model has to be properly scaled to avoid data overflow and ensure convergence of the solution algorithm. It is to be noticed, however, that this model may be rearranged such that it can be stored in the data RAM using fraction format without scaling.

Scaling is, however, necessary for avoiding overflow during Gauss elimination. This is evident if we consider that Gauss elimination manipulates each row of the coefficient matrix many times (multiplying one row by a constant and adding one to another). However, because a fixed-point data format is used, the scaling factor should be as small as possible to maximize the number of effective data bits. To solve this problem,a so-called dynamical scaling method has been applied: The local linear model is first scaled down by a small static factor. Then, during Gauss elimination, intermediate results are checked to see if overflow has occurred. Whenever it happens, the scaling factor is doubled.

VI. Experimental Results

The algorithms discussed so far have been successfully implemented in the digital signal processor DSP56001. The elimination of up to 15 harmonics without using any program or data memory expansion has been achieved.

The most important result might be the calculation time used by the DSP to solve harmonic elimination equations of different dimensions N (the number of switching angles). This is illustrated in Fig. 11 for N varying from 4 to 15 (the solid line). Notice that this is the time that the DSP needs for solving the equations for one iteration. The dashed line in Fig. 11

[1] N^2 sine functions in the Jacobian matrix $\boldsymbol{J}(\boldsymbol{a})$ and N^2 cosine functions in $\boldsymbol{g}(\boldsymbol{a})$.

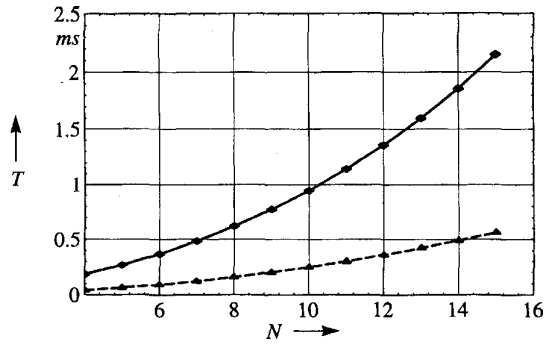

Fig. 11. On-line solution time for harmonic elimination equations of different dimension using a DSP56001.

represents the time for the evaluation of $2N^2$ trigonometrical functions based on the use of the sine wave table.

Measured pulse patterns generated by the modulator are shown in Fig. 12. The inverter is operated in a three-phase mode and is modulated to generate a normalized fundamental voltage $V_1 = 0.7$ with a fundamental frequency $f_1 = 50$ Hz. The switching frequency is 550 Hz such that the waveform has five switching angles in each quarter fundamental period ($N = 5$). As the result, four harmonics can be eliminated. This is evident from the spectrum shown in Fig. 12(b), where the fifth, seventh, eleventh, and thirteenth harmonics are not present. Triple-order harmonics such as the third, ninth, and fifteenth have no effect on the load and thus are not considered. For comparison, spectrum of the corresponding theoretical PWM waveform is also shown in Fig. 12(b) by the gray bars with dashed edges. Very good agreement between the measured and theoretical results can be observed.

Measured output current of the inverter supplying a three-phase induction motor is shown in Fig. 13. As the fifth, seventh, eleventh, and thirteenth voltage harmonics have been eliminated and triple-order harmonic current cannot flow, the lowest-order harmonic current is the seventeenth with the frequency $17 \times 50 = 850$ Hz. The magnitude of this harmonic is, however, small due to the higher impedance of the motor presented to higher-frequency harmonic voltages.

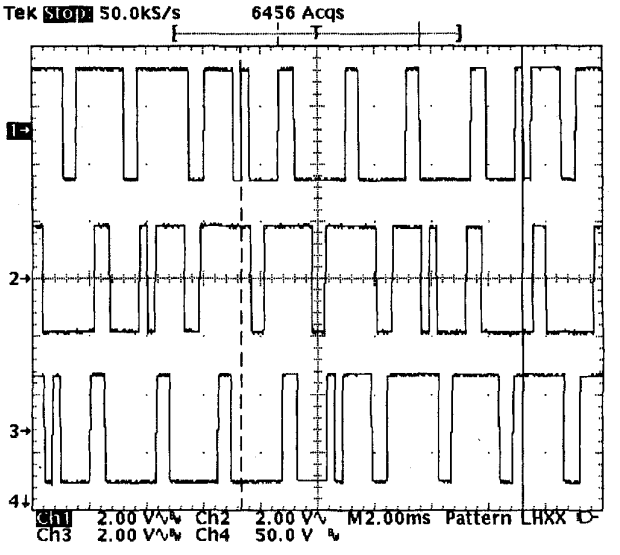

(a)

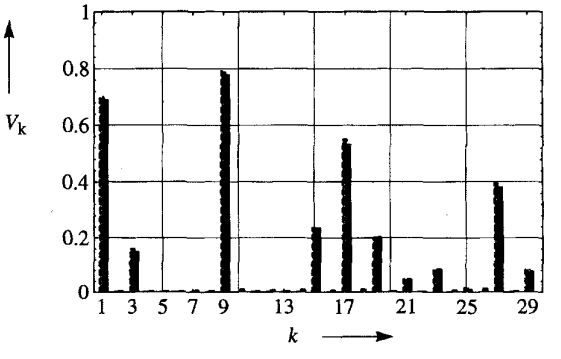

(b)

Fig. 12. (a) Measured output waveform of the modulator. (b) Spectrum of the measured waveform. The gray bars with dashed edges represent the corresponding theoretical spectrum determined using off-line solutions.

VII. Conclusion

It has been the major objective of this paper to verify through experimental implementations the feasibility of solving harmonic elimination problems on-line in real-time. As has been demonstrated, a digital signal processor of medium performance is usually sufficient for accomplishing this task. The success may be attributed to the novel design of assembly programs for the DSP as well as the development of new optimization equations and solution algorithms that suite the on-line solution. It is of course also a consequence of recent advances in digital electronic technology.

The results presented in this paper cleared up the doubt about the possibility of on-line solution of harmonic elimination problems. As previously discussed, on-line solution is more favorable, at least from the technical aspect, when both voltage and frequency regulations are required. It might also be attractive from the economical aspect, for that the solution of an optimal PWM problem can often be accomplished in conjunction with other tasks that necessitate also the use of a DSP, such that no extra DSP will be needed. Nevertheless, for a certain application, it is up to the system designer to compare the technical as well as economical merits of this and the conventional approaches with respect to his unique interests and to make a proper choice.

As theoretical results, the theorem presented in Section III and the subsequent discussion about three-phase inverters are also important as they address a fundamental question concerning the existence of harmonic elimination solutions and the solvability of equations.

The algorithms described in this paper would be useful for both on-line and off-line solutions of other optimal PWM problems, such as the minimization of harmonic current distortion or torque ripples.

Appendix—Proof of the Theorem

The Jacobian matrix of harmonic elimination equations for single-phase inverters can be decomposed into the multipli-

cation of two matrices as the matrix shown at the bottom of the page.

Since $\text{diag}\,(h_1, h_2, \cdots, h_N)$ is nonsingular, $\boldsymbol{J}(\boldsymbol{a})$ is singular if and only if $\boldsymbol{J}_1(\boldsymbol{a})$ is singular.

The *necessity* of the condition (7) for $\boldsymbol{J}_1(\boldsymbol{a})$ to be nonsingular is evident, for whenever $\alpha_i = 0$ or $\alpha_i = \alpha_j, 1 \le i, j \le N, \boldsymbol{J}_1(\boldsymbol{a})$ will have a zero column or two identical columns and is thus singular.

To prove that (7) is also sufficient for $\boldsymbol{J}_1(\boldsymbol{a})$ to be nonsingular, we notice first that a sine function of multiples of an angle can be represented by finite products as

$$\sin nx = n \sin x \prod_{i=1}^{(n-1)/2} \left(1 - \frac{\sin^2 x}{\sin^2 \dfrac{i\pi}{n}} \right), \qquad n = \text{odd}. \tag{11}$$

Suppose, by contradiction, that in spite of condition (7), matrix $\boldsymbol{J}_1(\boldsymbol{a})$ is singular. Then, there must exist a real vector $\boldsymbol{v} \in \boldsymbol{R}^N, \boldsymbol{v} \neq \boldsymbol{0}$, such that $v^T \boldsymbol{J}_1(\alpha) = \boldsymbol{0}$. This implies that

$$\sum_{i=1}^{N} v_i \sin\left[(2i-1)\alpha_k\right] = 0 \tag{12}$$

holds for each integer $k \in [1, N]$, where v_i is the ith element of vector $\boldsymbol{v}$. Using (11), (12) can be simplified to

$$\sum_{i=1}^{N} v_i (2i-1) \sin \alpha_k \prod_{j=1}^{i-1} \left(1 - \frac{\sin^2 \alpha_k}{\sin^2 \dfrac{j\pi}{2i-1}} \right) = \sin \alpha_k \left[\sum_{i=1}^{N} v_i (2i-1) \prod_{j=1}^{i-1} \left(1 - \frac{\sin^2 \alpha_k}{\sin^2 \dfrac{j\pi}{2i-1}} \right) \right] = 0. \tag{13}$$

Since $\alpha_k \neq 0$ such that $\sin \alpha_k \neq 0$, the above equation is equivalent to the following one in which $x = \sin^2 \alpha_k$

$$\sum_{i=1}^{N} v_i (2i-1) \prod_{j=1}^{i-1} \left(1 - \frac{x}{\sin^2 \dfrac{j\pi}{2i-1}} \right) = 0. \tag{14}$$

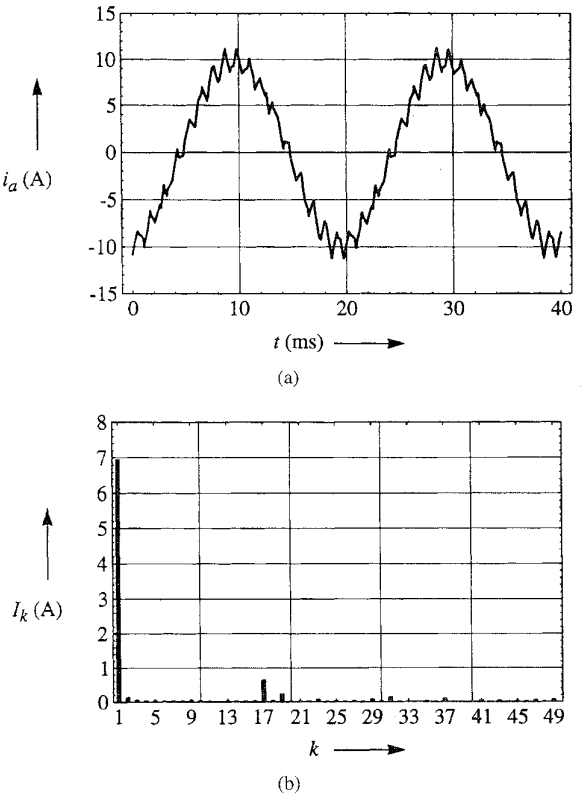

Fig. 13. (a) Measured phase current of the inverter supplying a three-phase induction motor. (b) Spectrum of the measured current.

We consider now (14) as an algebraic equation in variable x. Two observations that are contradictory with each other can then be made.

1) The fact that (12) holds for each $k \in [1, N]$ implies that (14) has N distinct solutions: $x_1 = \sin^2 \alpha_1, x_2 = \sin^2 \alpha_2, \cdots, x_N = \sin^2 \alpha_N$.[2]
2) However, since the left-hand side of (14) is a polynomial in x of degree $N-1$, (14) may have at most $N-1$ distinct solutions.

Since these contradictory observations are due to the assumption made above that $\boldsymbol{J}_1(\boldsymbol{a})$ is singular, we conclude that

[2]They are distinct since $\alpha_1, \alpha_2, \cdots, \alpha_{N-1}$, and α_N are assumed to be distinct from each other, as shown by (7).

$$\begin{aligned}
\boldsymbol{J}(\boldsymbol{a}) &= -\begin{bmatrix} h_1 \sin \alpha_1 & h_2 \sin \alpha_2 & \cdots & h_N \sin \alpha_N \\ h_1 \sin 3\alpha_1 & h_2 \sin 3\alpha_2 & \cdots & h_N \sin 3\alpha_N \\ h_1 \sin 5\alpha_1 & h_2 \sin 5\alpha_2 & \cdots & h_N \sin 5\alpha_N \\ \cdots & \cdots & & \cdots \\ h_1 \sin\left[(2N-1)\alpha_1\right] & h_2 \sin\left[(2N-1)\alpha_2\right] & \cdots & h_N \sin\left[(2N-1)\alpha_N\right] \end{bmatrix} \\
&= -\begin{bmatrix} \sin \alpha_1 & \sin \alpha_2 & \sin \alpha_N \\ \sin 3\alpha_1 & \sin 3\alpha_2 & \sin 3\alpha_N \\ \sin 5\alpha_1 & \sin 5\alpha_2 & \sin 5\alpha_N \\ \cdots & \cdots & \cdots \\ \sin\left[(2N-1)\alpha_1\right] & \cdots & \sin\left[(2N-1)\alpha_N\right] \end{bmatrix} \begin{bmatrix} h_1 & & \mathbf{0} \\ & h_2 & \\ & & \cdots \\ \mathbf{0} & & h_N \end{bmatrix} \\
&= -\boldsymbol{J}_1(\alpha)\,\text{diag}\,(h_1, h_2, \cdots, h_N)
\end{aligned}$$

matrix $\boldsymbol{J}_1(\boldsymbol{a})$ cannot be singular under (7). This completes the proof of the Theorem.

REFERENCES

[1] J. Holtz, "Pulsewidth modulation—A survey," in *Conf. Rec. PESC'92*, 1992, pp. 11–18.

[2] H. Grotstollen, "Line voltage modulation—A new possibility of PWM for three phase inverters," in *Conf. Rec. 1993 IEEE Industry Applications Socity 28th Ann. Meet.*, 1993, pp. 567–574.

[3] H. S. Patel and R. G. Hoft, "Generalized techniques of harmonic elimination and voltage control in thyristor inverters: Part I—Harmonic elimination," *IEEE Trans. Ind. Applicat.*, vol. IA-9, no. 3, pp. 310–317, May/June 1973.

[4] ———, "Generalized techniques of harmonic elimination and voltage control in thyristor inverters: Part II—Voltage control techniques," *IEEE Trans. Ind. Applicat.*, vol. IA-10, no. 5, pp. 666–673, Sept./Oct. 1974.

[5] P. Enjeti and J. F. Lindsay, "Solving nonlinear equations of harmonic elimination PWM in power control," *Electron. Lett.*, vol. 23, no. 12, pp. 656–657, June 4th, 1987.

[6] Q. Jiang, D. G. Holmes, and D. B. Giesner, "A method for linearising optimal PWM switching strategies to enable their computation on-line in real-time," in *Conf. Proc. 1991 IEEE Industry Applications Society Ann. Meet.*, Oct. 1991, pp. 819–825.

[7] R. J. Chance and J. A. Taufig, "A TMS32010 based near optimized pulse width modulated waveform generator," in *Conf. Proc. 1988 IEEE Industry Applications Society Ann. Meet.*, Oct. 1993, pp. 903–908.

[8] J. Sun and H. Grotstollen, "Solving nonlinear equations for selective harmonic eliminated PWM using predicted initial values," in *Conf. Proc. IECON'92*, Nov. 1992, pp. 259–264.

[9] *DSP56000/DSP56001 Digital Signal Processor, User's Manual,* Motorola Inc., 1990.

[10] J. Sun, "Optimal pulsewidth modulation techniques for high power voltage-source inverters," Ph. D. thesis, Univ. of Paderborn, Germany, 1995.

Jian Sun (M'95) was born in Jiangsu, People's Republic of China (PRC), in 1964. He received the B.Eng. degree from Nanjing Institute of Aeronautics (now Nanjing University of Aeronautics and Astronautics), Nanjing, PRC, in 1984, the M.Eng. degree from Beijing University of Aeronautics and Astronautics, Beijing, PRC, in 1989, and the Dr.-Ing. degree from the University of Paderborn, Germany, in 1995, all in electrical engineering. He was a Ph.D. student at Beijing University of Aeronautics and Astronautics from 1989 to 1991.

From 1984 to 1987 he was an Electrical Engineer with Xian Aircraft Company, Xian, PRC. In 1991 he joined the Institute for Power Electronics and Electrical Drives, University of Paderborn, Germany, and worked toward his Dr.-Ing. degree. He is presently Research Associate with the University of Paderborn. His research interests include power electronic system modeling and simulation, high-performance pulsewidth modulation, active power filtering, and high-power-factor ac/dc conversion.

Stephan Beineke was born in 1967 in Hoexter, Germany. He received the M.S. degree in electrical engineering from University of Paderborn, Germany, in 1994. His master thesis was about the real-time implementation of harmonic elimination.

Since 1994 he has been working as Ph.D. student at University of Paderborn in the field of electrical drives, where he is investigating speed and position control of drives, including identification of the mechanics, with neural-, fuzzy-, and observer-based methods.

Horst Grotstollen studied in Germany and received the Ing.-grad., the Dipl.-Ing. and the doctorate degrees in electrical engineering from Staatliche Ingenieurschule Duisburg in 1960, from Rheinisch-Westfaelische Technische Hochschule Aachen in 1965, and from Technische Universitaet Berlin in 1972, respectively. He habilitated at the University of Erlangen-Nuernberg in 1982.

He joined AEG in 1965, where he developed electrical servo drives at the Frankfurt Research Center from 1965 to 1970 and drive problems at the Department of Industrial Equipment from 1970 to 1973. He was with the Chair for Electrical Drives of the University of Erlangen-Nuernberg since 1973, as a Chief Engineer, where he taught courses on electrical machines and power electronics while conducting researches on servo drives with permanent magnet synchronous motors. Since 1981 he has been Professor at the University of Paderborn. His research interests are digital control of ac drives and switch-mode power supplies.